Weierstraß–Institut
für Angewandte Analysis und Stochastik

im Forschungsverbund Berlin e.V.

Preprint ISSN 0946 – 8633

Initial and Boundary Value Problems of Hyperbolic Heat Conduction

Wolfgang Dreyer, Matthias Kunik

submitted: 25. September 1998

Weierstrass Institute
for Applied Analysis
and Stochastics
Mohrenstrasse 39
D–10117 Berlin
Germany
E-Mail: dreyer@wias-berlin.de
E-Mail: kunik@wias-berlin.de

Preprint No. 438
Berlin 2000

1991 Mathematics Subject Classification. 80-99, 35L15, 35L20, 35L65, 35L67.

Key words and phrases. Heat transfer, initial and boundary value problems for a hyperbolic system, shock waves, kinetic theory.

Edited by
Weierstraß–Institut für Angewandte Analysis und Stochastik (WIAS)
Mohrenstraße 39
D — 10117 Berlin
Germany

Fax: + 49 30 2044975
E-Mail (X.400): c=de;a=d400-gw;p=WIAS-BERLIN;s=preprint
E-Mail (Internet): preprint@wias-berlin.de
World Wide Web: http://www.wias-berlin.de/

Abstract

This is a study on the initial and boundary value problem of a symmetric hyperbolic system which is related to the conduction of heat in solids at low temperatures. The nonlinear system consists of a conservation equation for the energy density e and a balance equation for the heat flux Q_i, where e and Q_i are the four basic fields of the theory. The initial and boundary value problem that uses exclusively prescribed boundary data for the energy density e is solved by a new kinetic approach that was introduced and evaluated by Dreyer and Kunik in [1], [2] and Pertame [3]. This method includes the formation of shock fronts and the broadening of heat pulses. These effects cannot be observed in the linearized theory, as it is described in [4].

The kinetic representations of the initial and boundary value problem reveal a peculiar phenomenon. To the solution there contribute integrals containing the initial fields $e_0(x), Q_0(x)$ as well as integrals that need knowledge on energy *and* heat flux at a boundary. However, only one of these quantities can be controlled in an experiment. When this ambiguity is removed by continuity conditions, it turns out that after some very short time the energy density and heat flux are related to the initial data according to the Rankine Hugoniot relation.

1 Introduction

Heat conduction processes are usually described by a parabolic system. It results from a diffusion law, where the heat flux is proportional to the temperature gradient. That constitutive law implies the paradox of heat conduction whereupon heat may transverse a body with infinite speed. This fact is not acceptable from a physical point of view. In most technical processes, in particular at room temperature, those modes that propagate with infinite speed suffer a considerable damping and are thus not observable. However, there are cases where either the damping of a heat pulse is quite low or where its travel distance is so small that the transit time is an observable quantity. In those cases the parabolic system has to be replaced by the physically justified hyperbolic system of heat conduction. A comprehensive study of many phenomena which appear in the temperature range between $5^\circ K$ and $20^\circ K$ is described by DREYER and STRUCHTRUP in the review article [4], see also the textbook on Rational Extended Thermodynamics by MÜLLER and RUGGERI [5]. In that range heat conduction of crystalline solids must be considered as the motion of phonons which may interact with lattice impurities and with each other.

DREYER and STRUCHTRUP report on special circumstances that are met in quite pure crystals at not too low temperature, where the state of a crystal is sufficiently described by only four thermodynamic fields as the basic variables. These are the energy density e, or the temperature T, and the heat flux $\mathbf{Q} = (Q_i)_{i=1,2,3}$. DREYER and STRUCHTRUP give the necessary restrictions that must be met in the experiment for the physical applicability of this assumption. Independent from these problems we consider in this paper the resulting system of four field equations in its own right, because it exhibits already several serious mathematical aspects of the initial and boundary value problem.

The resulting system of field equations is of the symmetric hyperbolic type. In this paper we consider mainly this system in one space dimension and solve its pure initial value problem as well as the initial and boundary value problem by using kinetic representations for the unknown fields. The system consists of a conservation law for the energy density e and of a balance law for the heat flux $\mathbf{Q}$, and it is derived by averaging the BOLTZMANN-PEIERLS equation. The closure problem is solved by the *Maximum Entropy Principle* [6].

The BOLTZMANN-PEIERLS equation describes the evolution of the phase density $f(t,\mathbf{x},\mathbf{k})$. $f(t,\mathbf{x},\mathbf{k})\, d^3x\, d^3k$ is interpreted as the number of phonons which are at time t in a small spatial volume element d^3x at location $\mathbf{x}$ and which have a momentum $\hbar\,\mathbf{k}$ in the range d^3k. $\mathbf{k}$ denotes the wave vector and $\hbar$ is PLANCKs constant. For more details we refer the reader to [4]. The BOLTZMANN-PEIERLS equation reads

$$\frac{\partial f}{\partial t} + \frac{\partial \omega}{\partial k_k}\frac{\partial f}{\partial x_k} \;=\; \zeta(f)\,. \tag{1.1}$$

In a real crystal there are three phonon modes and thus there are three phase densities corresponding to two transversal modes and one longitudinal mode. In [4] it is described that for simplicity one can replace the actual crystal by a so called DEBYE solid, which is characterized by a single mode only. In addition the assumed dispersion relation between the phonon frequency ω and the wave vector $\mathbf{k}$ is given by

$$\omega \;=\; c\,|\mathbf{k}|\,. \tag{1.2}$$

Here the constant Debye velocity c is related to a mean of the two transversal and longitudinal sound speeds of the actual crystal.

The collision term $\zeta(f)$ in (1.1) describes the so called R- and N-processes. R-processes include interactions of phonons with lattice impurities which destroy the periodicity of the crystal, while N-processes can be interpreted as phonon-phonon interactions which are due to deviations of the harmonicity of the crystal forces. N-processes conserve phonon momentum while R-processes do not. Both kinds of processes conserve the energy of the phonons.

In section 2 we derive the equations of balance for the energy density e and the heat flux $\mathbf{Q}$ as transfer equations from the BOLTZMANN-PEIERLS equation. The basic fields and their corresponding fluxes turn out to be given by the following moments of the phase density f:

$$
\begin{aligned}
e(t, \mathbf{x}) &= \hbar c \int_{-\infty}^{\infty} |\mathbf{k}| f(t, \mathbf{x}, \mathbf{k}) \; d^3\mathbf{k}, \\
Q_i(t, \mathbf{x}) &= \hbar c^2 \int_{-\infty}^{\infty} k_i f(t, \mathbf{x}, \mathbf{k}) \; d^3\mathbf{k}, \\
N_{ik}(t, \mathbf{x}) &= \hbar c \int_{-\infty}^{\infty} \frac{k_i k_k}{|\mathbf{k}|} f(t, \mathbf{x}, \mathbf{k}) \; d^3\mathbf{k}.
\end{aligned}
\tag{1.3}
$$

N_{ik} appears as a flux in the equation of balance for the heat flux and it does not occur among the variables e and $\mathbf{Q}$. N_{ik} will be related to the variables by the *Maximum Entropy Principle.* It states that the phase density $f = f^{(4)}$ that corresponds to the macroscopic knowledge of the four fields e and $\mathbf{Q}$, is obtained by maximizing the entropy density under the constraints of prescribed fields e and $\mathbf{Q}$.

In order to evaluate this principle one needs, however, a kinetic representation of the entropy density which will be given in section 3.

In section 4 we present a modified BOLTZMANN-PEIERLS equation without the collision term. However, it will lead to the same system of field equations that results from the original BOLTZMANN-PEIERLS equation. The solution of the modified BOLTZMANN-PEIERLS equation is easily obtained and implies a solution of the non-linear hyperbolic system.

For example, the pure initial value problem may be solved as follows: At any time the moments e and $\mathbf{Q}$ are determined by a phase density f that results from the modified BOLTZMANN-PEIERLS equation for the initial condition $f(t_0, \mathbf{x}, \mathbf{k}) = f^{(4)}(t_0, \mathbf{x}, \mathbf{k})$. Here the initial phase density maximizes the entropy for given initial data $e(t_0, \mathbf{x})$ and $\mathbf{Q}(t_0, \mathbf{x})$ as constraints.

At the next time $t_1 = t_0 + \tau_M$, where $\tau_M > 0$ is a given time step size, the moments $e(t_1, \mathbf{x})$ and $\mathbf{Q}(t_1, \mathbf{x})$ constructed from the phase density $f(t_0, \mathbf{x}, \mathbf{k})$ above are used as the new initial data. The procedure will be repeated for the subsequent times $t_1 < t_2 < t_3 < \ldots$. This kinetic approach is described in section 5, which ends with two explicit examples: The first example compares the numerical results with the analytical predictions for the propagation of a single shock front taken from [6]. In the second example we consider the interaction of two heat pulses.

In section 6 we extend the representation formulas for the pure initial value problem so that boundary conditions are also included. Here we are confronted with a serious problem. From an experimental point of view the energy density e and the heat flux $\mathbf{Q}$ cannot be given simultaneously at a boundary, either e or $\mathbf{Q}$ can be controlled. We will show that this ambiguity can be removed by three continuity conditions. Those conditions lead to the surprising result that after a very short time the solution assumes boundary data for e and $\mathbf{Q}$ that are related to the initial data by the so-called Rankine-Hugoniot shock-condition. Up to now this observation is only supported by numerical tests. A careful study of this astonishing phenomenon is left for a future investigation. Instead we present here three explicit examples for the initial and boundary value problem: The first two deal with a rectangular pulse and a cosine disturbance, respectively, as boundary data for the energy density e. We consider the cases of high and zero damping. In a third example we consider the reflection of a heat pulse at the boundary and show in the linear limit that the analytical solution agrees with the numerical result.

Another interesting result regards the speed of the fastest shock front which runs into equilibrium. It turned out to be apparently larger than $\frac{c}{\sqrt{3}}$. Furthermore, we observe a broadening of an original heat pulse at later times. Both phenomena cannot be obtained from the linearized four field system, as explained in [4].

Finally we consider the boundary-value problem for a stationary heat- conduction process between two boundaries and calculate its analytical solution when either the energy density is prescribed at both boundaries, or the energy density is given at one boundary and the heat flux at the other.

2 Equations of Balance for Energy and Heat Flux

The Boltzmann-Peierls equation for the phonon phase density

$$\frac{\partial f}{\partial \tau} + c\,\frac{k_i}{|\mathbf{k}|}\frac{\partial f}{\partial x_i} = \zeta(f) \tag{2.1}$$

implies infinitely many equations of balance for moments of the phase density. We are only interested in the first four equations which are obtained by multiplication of (2.1) by $\hbar c|\mathbf{k}|$ and $\hbar c^2\,k_i$ and integration over $\mathbf{k}$. There results the equations of balance for the energy density e and the heat flux Q_i

$$\begin{aligned} \frac{\partial e}{\partial \tau} + \frac{\partial Q_k}{\partial x_k} &= \hbar\, c \int_{-\infty}^{+\infty} |\mathbf{k}|\,\zeta(f)\, d^3\mathbf{k}\ , \\ \frac{\partial Q_i}{\partial \tau} + \frac{\partial (c^2\, N_{ik})}{\partial x_k} &= \hbar\, c^2 \int_{-\infty}^{+\infty} k_i\,\zeta(f)\, d^3\mathbf{k}\ . \end{aligned} \tag{2.2}$$

When we consider e and Q_i as the (macroscopic) basic variables for which initial and boundary value problems have to be solved, we must close the system (2.2) so that the flux N_{ik} and the production terms on the right hand sides are related to the variables.

This objective is achieved by applying the *Maximum Entropy Principle,* which gives, as shown in the next section, a phase density of the form

$$f^{(4)}(t,\mathbf{x},\mathbf{k}) = w^{(4)}(e(t,\mathbf{x}),\mathbf{Q}(t,\mathbf{x}),\mathbf{k}). \tag{2.3}$$

Here the (t,x) dependence is in fact a dependence on the variables $e(t,x)$ and $Q_i(t,x)$.

Note that this function is no longer a solution of the Boltzmann-Peierls equation. But nevertheless we will keep equations (2.2) and replace f by $f^{(4)}$. It can be shown, see [7] and [8], that the resulting closed system is of symmetric hyperbolic type and has a convex extension.

3 The Maximum Entropy Principle for Four Fields

In this section we maximize the entropy of the phonon-Bose gas under the constraints of given energy density and heat flux. The entropy density h and the entropy flux Φ_k of the phonon-Bose gas are given according to the kinetic theory [4] as

$$\begin{aligned} h &= -k_B \int_{-\infty}^{\infty} \left[f \ln(\frac{f}{y}) - y(1+\frac{f}{y}) \ln(1+\frac{f}{y}) \right] \, d^3\mathbf{k} \ , \\ \Phi_k &= -k_B \int_{-\infty}^{\infty} c \frac{\mathbf{k}_k}{|\mathbf{k}|} \left[f \ln(\frac{f}{y}) - y(1+\frac{f}{y}) \ln(1+\frac{f}{y}) \right] \, d^3\mathbf{k} \ . \end{aligned} \tag{3.1}$$

$k_B = 1,38 \cdot 10^{-23} J/K$ is BOLTZMANN's constant and $y = 3/8\pi^3$.

For the maximization of h with respect to f under the given constraints

$$e = \hbar c \int_{-\infty}^{\infty} |\mathbf{k}| f \ d^3\mathbf{k} \ , \ Q_i = \hbar c^2 \int_{-\infty}^{\infty} k_i f \ d^3\mathbf{k} \ , \tag{3.2}$$

we may introduce LAGRANGE multipliers Λ_0 corresponding to e and Λ_i corresponding to Q_i and maximize

$$G = \frac{1}{k_B} h - \Lambda_0 \left[\hbar c \int_{-\infty}^{\infty} |\mathbf{k}| f \ d^3\mathbf{k} - e \right] - \Lambda_i \left[\hbar c^2 \int_{-\infty}^{\infty} k_i f \ d^3\mathbf{k} - Q_i \right] \tag{3.3}$$

without constraints. The resulting phase density reads

$$f^{(4)}(t, \mathbf{x}, \mathbf{k}) = \frac{y}{\exp(\Sigma) - 1} \ , \tag{3.4}$$

with

$$\Sigma(t, \mathbf{x}, \mathbf{k}) = \hbar c \left(|\mathbf{k}| \Lambda_0(t, \mathbf{x}) + c k_i \Lambda_i(t, \mathbf{x}) \right) \qquad , \tag{3.5}$$

$$\Lambda_0 = \gamma \frac{(\frac{F}{e})^{\frac{1}{4}}}{(4-F)^{\frac{3}{4}}} \ , \ \Lambda_i = -\frac{\gamma}{4} \frac{(\frac{F}{e})^{\frac{5}{4}}}{(4-F)^{\frac{3}{4}}} Q_i \ , \ F = \frac{6}{1 + \sqrt{1 - \frac{3}{4} \left(\frac{|\mathbf{Q}|}{ce} \right)^2}} \ , \ \gamma = \left(\frac{4\pi^5 y}{45 h^3 c^3} \right)^{\frac{1}{4}} . \tag{3.6}$$

For experimental purposes it is sometimes useful to use the (absolute) temperature T instead of the energy density e. Both quantities are related to each other so that the STEFAN-BOLTZMANN law for phonons is established, viz.

$$T = \frac{1}{k_B}\left(\frac{10\hbar^3 c^3}{\pi^2} e\right)^{\frac{1}{4}} . \tag{3.7}$$

Obviously, the heat flux must be zero in equilibrium, and the *equilibrium phase-density* $f^{(1)}$ thus reads

$$f^{(1)}(t,\mathbf{x},\mathbf{k}) = \frac{y}{\exp(\Sigma)-1} \ , \ \Sigma(t,\mathbf{x},\mathbf{k}) = \frac{\hbar c|\mathbf{k}|}{k_B T(t,\mathbf{x})}. \tag{3.8}$$

Formally $f^{(1)}$ can be obtained from $f^{(4)}$ by setting Q_i equal to zero.

In the kinetic theory of phonons it can be shown [4] that the collision term of the Boltzmann-Peierls equation may be approximated by

$$\zeta(f) = \frac{f^{(1)} - f}{\tau_R} + \frac{f^{(4)} - f}{\tau_N} \ , \tag{3.9}$$

which represents a good approximation to the quantum mechanically based true collision production. The collision function ζ contains two relaxation times τ_R and τ_N. τ_R describes resistive processes which include interaction of phonons with lattice impurities, while the second relaxation time τ_N takes care of phonon-phonon interactions which are due to the non- harmonicity of the lattice.

When the thermodynamic state is described by the four fields e and Q_i only, as it is done here, it follows that the τ_N part drops out from the collision integral and the applicability of the current theory is thus restricted to the limit $\tau_N \to 0$. Thus heat conduction is only due to second sound and to diffusion. For the general case we refer the reader to the review article by Dreyer and Struchtrup [4]. Here we are mainly interested in the initial and boundary value problem for the four field system, which now reads

$$\begin{aligned} \frac{\partial e}{\partial \tau} + \frac{\partial Q_k}{\partial x_k} &= 0 \ , \\ \frac{\partial Q_i}{\partial \tau} + \frac{\partial (c^2 N_{ik})}{\partial x_k} &= -\frac{1}{\tau_R} Q_i \ , \\ N_{ik} = \frac{1}{3} e\, \delta_{ik} &+ \frac{1}{2} e(3\chi - 1)\frac{Q_{<i}Q_{k>}}{Q^2} \ , \end{aligned} \tag{3.10}$$

where χ is the so called Eddington-factor

$$\chi = \frac{5}{3} - \frac{4}{3}\sqrt{1 - \frac{3}{4}\left(\frac{Q}{c\,e}\right)^2} \ . \tag{3.11}$$

By use of $f^{(4)}$ we may also calculate the entropy density h, the entropy flux ϕ_k and the entropy production σ as local functions of e and $\mathbf{Q}$, which turn out to be (see [6] and [9])

$$\begin{aligned} h &= \left(\frac{2a}{3}\right)^{\frac{1}{4}} e^{\frac{3}{4}}(3-\chi)^{\frac{1}{2}}(1-\chi)^{\frac{1}{4}}, \\ \phi_k &= 2\left(\frac{2a}{3}\right)^{\frac{1}{4}} e^{-\frac{1}{4}}(3-\chi)^{-\frac{1}{2}}(1-\chi)^{\frac{1}{4}}\, Q_k, \\ \sigma &= -\frac{k_B}{\tau_R}\sum_{i=1}^{3}\Lambda_i Q_i\ , \quad a := -\frac{\pi^2}{10}\, k_B^4/(\hbar^3 c^3)\ . \end{aligned} \tag{3.12}$$

Entropy density, entropy flux and entropy production are related to each other by an additional balance law, viz.

$$\frac{\partial h}{\partial t} + \frac{\partial \phi_k}{\partial x_k} = \sigma \geq 0\ . \tag{3.13}$$

Furthermore, it follows that the entropy production is zero in equilibrium and otherwise positive [8].

4 A Modified Kinetic Model

Note that we already abandoned the BOLTZMANN-PEIERLS equation by using the Maximum Entropy Principle for the determination of the phase density. In other words: the hyperbolic system (3.10) does not constitute a solution of the BOLTZMANN-PEIERLS equation. Now we proceed one step further in the same direction and replace the Boltzmann-Peierls equation by a much more simpler equation, which however leads in fact to the solution of the hyperbolic system (3.10). To this end we start at time t_0 with initial data $e_0(\mathbf{x}) = e(t_0, \mathbf{x})$ and $\mathbf{Q}_0(\mathbf{x}) = \mathbf{Q}(t_0, \mathbf{x})$, and use as the initial phase density

$$f(t_0, \mathbf{x}, \mathbf{k}) = w^{(4)}(e_0(\mathbf{x}), \mathbf{Q}_0(\mathbf{x}), \mathbf{k})\ . \tag{4.1}$$

For $t > t_0$ we define the phase density f according to

$$f(t_0 + \tau, \mathbf{x}, \mathbf{k}) = f(t_0, \mathbf{x} - c\,\psi(\tau)\frac{\mathbf{k}}{|\mathbf{k}|}, \mathbf{k})\ \ , \tag{4.2}$$

where the bounded function $\psi(\tau)$ is defined for $\tau \geq 0$ as

$$\psi(\tau) = \tau_R\,(1 - \exp(-\frac{\tau}{\tau_R})) < \tau_R \quad . \tag{4.3}$$

We conclude that the phase density (4.2) satisfies the collision-free kinetic equation

$$\frac{\partial f}{\partial \tau} + \dot{\psi}(\tau)\, c \frac{k_i}{|\mathbf{k}|} \frac{\partial f}{\partial x_i} = 0 \ . \tag{4.4}$$

However, the hyperbolic system (3.10), and in particular the non-vanishing right-hand side of $(3.10)_2$ will now turn out to be a consequence of (4.2) and (4.4).

This will be established by a redefinition of the moments (1.3). While the energy density e will be defined as before, but with the phase density (4.2), the heat flux Q_i and its flux N_{ik} involve in addition the functions $\dot{\psi}(\tau)$ and $\dot{\psi}^2(\tau)$ as new time-dependent factors:

$$\begin{aligned} e(t_0+\tau,\mathbf{x}) &= \hbar c \int_{-\infty}^{\infty} |\mathbf{k}| f(t_0+\tau,\mathbf{x},\mathbf{k})\ d^3\mathbf{k}, \\ Q_i(t_0+\tau,\mathbf{x}) &= \hbar c^2 \dot{\psi}(\tau) \int_{-\infty}^{\infty} k_i f(t_0+\tau,\mathbf{x},\mathbf{k})\ d^3\mathbf{k}, \\ N_{ik}(t_0+\tau,\mathbf{x}) &= \hbar c \dot{\psi}^2(\tau) \int_{-\infty}^{\infty} \frac{k_i k_k}{|\mathbf{k}|} f(t_0+\tau,\mathbf{x},\mathbf{k})\ d^3\mathbf{k}. \end{aligned} \tag{4.5}$$

These definitions imply equations of balance that have the same structure as the corresponding hyperbolic system (3.10)

$$\begin{aligned} \frac{\partial e}{\partial \tau} + \frac{\partial Q_k}{\partial x_k} &= 0, \\ \frac{\partial Q_i}{\partial \tau} + \frac{\partial (c^2\, N_{ik})}{\partial x_k} &= -\frac{1}{\tau_R} Q_i. \end{aligned} \tag{4.6}$$

It is important to note that in contrast to the local system (3.10), the system (4.6) is non-local in time and space. In the next two sections we will show how the representations (4.5) can be used in order to solve the initial and boundary-value problem for the local hyperbolic system (3.10).

5 The Pure Initial Value Problem (IVP)

5.1 Kinetic solution of the IVP

In order to solve the initial value problem for the nonlinear four field system (3.10), we start at a fixed time t_0 with given initial data e_0 for the energy density and $\mathbf{Q}_0$ for the heat flux. Next we consider the finite time interval $t_0 \le t \le t_0 + \tau_M$ for a given time step τ_M, where we let the phase density $f(t_0+\tau,\mathbf{x},\mathbf{k})$ develop according to (4.2), viz. $f(t_0, \mathbf{x} - c\,\psi(\tau)\frac{\mathbf{k}}{|\mathbf{k}|}, \mathbf{k})$.

At time $t_0+\tau_M$, we calculate the fields $e(t_0+\tau_M,\cdot)$ and $\mathbf{Q}(t_0+\tau_M,\cdot)$ from (4.5) with $f(t_0, \mathbf{x} - c\,\psi(\tau_M)\frac{\mathbf{k}}{|\mathbf{k}|}, \mathbf{k})$. For $t > t_0 + \tau_M$ we let the phase density develop according to $f(t_0+\tau_M, \mathbf{x} - c\,\psi(\tau)\frac{\mathbf{k}}{|\mathbf{k}|}, \mathbf{k})$, using the new initial data $e(t_0+\tau_M,\cdot)$, $\mathbf{Q}(t_0+\tau_M,\cdot)$. At time $t_0+2\tau_M$ we calculate the fields $e(t_0+2\tau_M,\cdot)$, $\mathbf{Q}(t_0+2\tau_M,\cdot)$ from (4.5), and so on.

In summary the procedure runs as follows. To initialize the scheme we start with

- Bounded and integrable initial data for $\mathbf{x} \in I\!R^3$ at time $t=0$: $e(0,\mathbf{x}) = e_0(\mathbf{x}) \geq \epsilon > 0$, $\mathbf{Q}(0,\mathbf{x}) = \mathbf{Q}_0(\mathbf{x})$ under the restriction $|\mathbf{Q}| < c\,e$.
- A fixed time step $\tau_M > 0$, so that the maximization of entropy is carried out at the equidistant times $t_n = n\tau_M$, $n = 0, 1, 2, \ldots$:

$$
\begin{aligned}
e(t_n+\tau,\mathbf{x}) &= \hbar\, c \int_{-\infty}^{+\infty} |\mathbf{k}| f_n(\mathbf{y},\mathbf{k})\; d^3\mathbf{k}, \\
Q_i(t_n+\tau,\mathbf{x}) &= \hbar\, c^2 \exp(-\frac{\tau}{\tau_R}) \int_{-\infty}^{+\infty} k_i\, f_n(\mathbf{y},\mathbf{k})\; d^3\mathbf{k},
\end{aligned}
\tag{5.1}
$$

where the phase-density at the maximization time t_n reads

$$
f_n(\mathbf{y},\mathbf{k}) = w^{(4)}(e(t_n,\mathbf{y}), \mathbf{Q}(t_n,\mathbf{y}), \mathbf{k}) \;,\; \mathbf{y} = \mathbf{x} - c\,\psi(\tau)\frac{\mathbf{k}}{|\mathbf{k}|} \;. \tag{5.2}
$$

In the following we are only interested in one-dimensional solutions, which do not depend on x_2 and x_3. In this case we may choose polar-coordinates for the $\mathbf{k}$-integration, and, using (3.4), (3.5),(3.6), the three-dimensional integral representations reduce to one-dimensional integrals

$$
\begin{aligned}
e(t_n+\tau,x) &= \frac{3}{2}\int_{-1}^{+1} \frac{e\,(4-F)^3}{F\,(1-\frac{F}{4}\frac{Q\,\nu}{c\,e})^4}(t_n,y)\; d\,\nu \;, \\
Q(t_n+\tau,x) &= \frac{3}{2}\, c\, \exp(-\frac{\tau}{\tau_R}) \int_{-1}^{+1} \frac{e\,(4-F)^3\,\nu}{F\,(1-\frac{F}{4}\frac{Q\,\nu}{c\,e})^4}(t_n,y)\; d\,\nu
\end{aligned}
\tag{5.3}
$$

with

$$
y = x - c\,\psi(\tau)\,\nu \quad , \quad F = \frac{6}{1+\sqrt{1-\frac{3}{4}\left(\frac{Q}{c\,e}\right)^2}} \;. \tag{5.4}
$$

In the explicit cases dealt with in the next sections we could observe that a unique solution of the hyperbolic system (3.10) including all possible shocks is established by the kinetic procedure in the limit $\tau_M \to 0$. The one-dimensional weak form of (3.10) for discontinuous solutions is given in the following subsection.

5.2 Riemannian initial data and shock condition

We consider now a single shock front which propagates into a region of thermal equilibrium. In this case one can explicitely solve the Rankine-Hugoniot conditions for a single shock solution, and this was already done by Dreyer & Seelecke in [6]. In the following we will use their results to reach two objectives. In this section we will compare our numerical results with their analytical predictions. In section 6 we will observe that in general the Rankine-Hugoniot shock conditions may serve to remove an ambiguity appearing in the solution formulas of the initial and boundary-value problems.

As before, we restrict ourselves to the one-dimensional case and write down the weak formulation of the four-field system (3.10) with a convex region Ω in space and time:

$$\begin{aligned} &\int_{\partial\Omega} (e\,dx \;-\; Q\,dt) = 0\ , \\ &\int_{\partial\Omega} (Q\,dx \;-\; c^2\,e\chi\,dt) = -\tfrac{1}{\tau_R} \iint_{\Omega} Q\;dt\,dx\ , \\ &\chi \;=\; \tfrac{5}{3} - \tfrac{4}{3}\sqrt{1-\tfrac{3}{4}\left(\tfrac{Q}{c\,e}\right)^2}\ . \end{aligned} \tag{5.5}$$

Next we prescribe RIEMANNian initial data

$$e_0(x) = \begin{cases} e_- & ,\quad x \le 0 \\ e_+ & ,\quad x > 0 \end{cases}\ , \qquad Q_0(x) = \begin{cases} Q_- & ,\quad x \le 0 \\ Q_+ & ,\quad x > 0 \end{cases}\ . \tag{5.6}$$

In order to guarantee that only a single shock solution occurs, we introduce the shock-parameter $X = e_-/e_+ > 1$, which determines the strength of the shock. Then we choose the equilibrium state $e_+ > 0$, $Q_+ = 0$ to the right of the shock and calculate the state e_-, Q_- to the left of the shock according to the Dreyer-Seelecke condition

$$e_- = Xe_+\ , \quad Q_- = (X-1)e_+\,\frac{c}{\sqrt{3}}\sqrt{\frac{3\sqrt{X}-1}{\sqrt{X}+1}}\ . \tag{5.7}$$

The shock speed $V_s > 0$ is also taken from [6] and reads

$$V_s = \frac{c}{\sqrt{3}}\sqrt{\frac{3\sqrt{X}-1}{\sqrt{X}+1}}\ . \tag{5.8}$$

Note that the condition $X > 1$ selects the single shock solution from other possible solutions of the RIEMANN problem and implies that always $V_s > c/\sqrt{3}$. We will see that instead of a single shock a more complicated solution with a rarefaction wave will appear for an initial data that do not satisfy the condition $X > 1$.

Sometimes it is useful to define another shock parameter via the shock speed. The new shock parameter gives the deviation from c and is defined as

$$\alpha = \frac{V_s}{c} = \frac{1}{\sqrt{3}} \sqrt{\frac{3\sqrt{X} - 1}{\sqrt{X} + 1}} \; . \tag{5.9}$$

Note that V_s is restricted to the range $c/\sqrt{3} < V_s < c$. Using α, with $1/\sqrt{3} < \alpha < 1$, instead of X, the Dreyer-Seelecke condition reads

$$e_- = \frac{1}{9} e_+ \frac{(3\alpha^2 + 1)^2}{(1-\alpha)^2} \; , \quad Q_- = \frac{8}{9} c e_+ \alpha \frac{3\alpha^2 - 1}{1 - \alpha^2} \; . \tag{5.10}$$

In the following we set $c = 1$ for simplicity.

Figure 1 shows for Riemannian initial data of type (5.6) three initial value problems for the two fields energy density e and heat flux Q. The space region is $-0.5 \le x \le 0.5$ and the time is restricted to $0 \le t \le 0.5$. The first row displays a single shock solution resulting from the initial data $e_+ = 1$, $Q_+ = 0$, $X = 2$ for large relaxation time $\tau_R = 8$. The light and dark colours correspond to small and large values of the fields, respectively, ranging from $e_{min} = 1$, $Q_{min} = 0$ (light colour) to $e_{max} = 2$, $Q_{max} = 0.67$ (dark colour).

The second row displays the same initial value problem but for small relaxation time $\tau_R = 0.2$. This value corresponds to a dominant right-hand side and causes a strong diffusion of the original shock front. The extreme values of e and Q are the same as before.

The third row displays the development of initial conditions that violate the Dreyer-Seelecke shock condition $X > 1$. Here the initial data result from $e_+ = 1$, $Q_+ = 0$, $X = 0.3$ for a large relaxation time $\tau_R = 8$. The extreme values of the fields range from $e_{min} = 0.3$, $Q_{min} = -0.26$ (light colour) to $e_{max} = 1$, $Q_{max} = 0$ (dark colour).

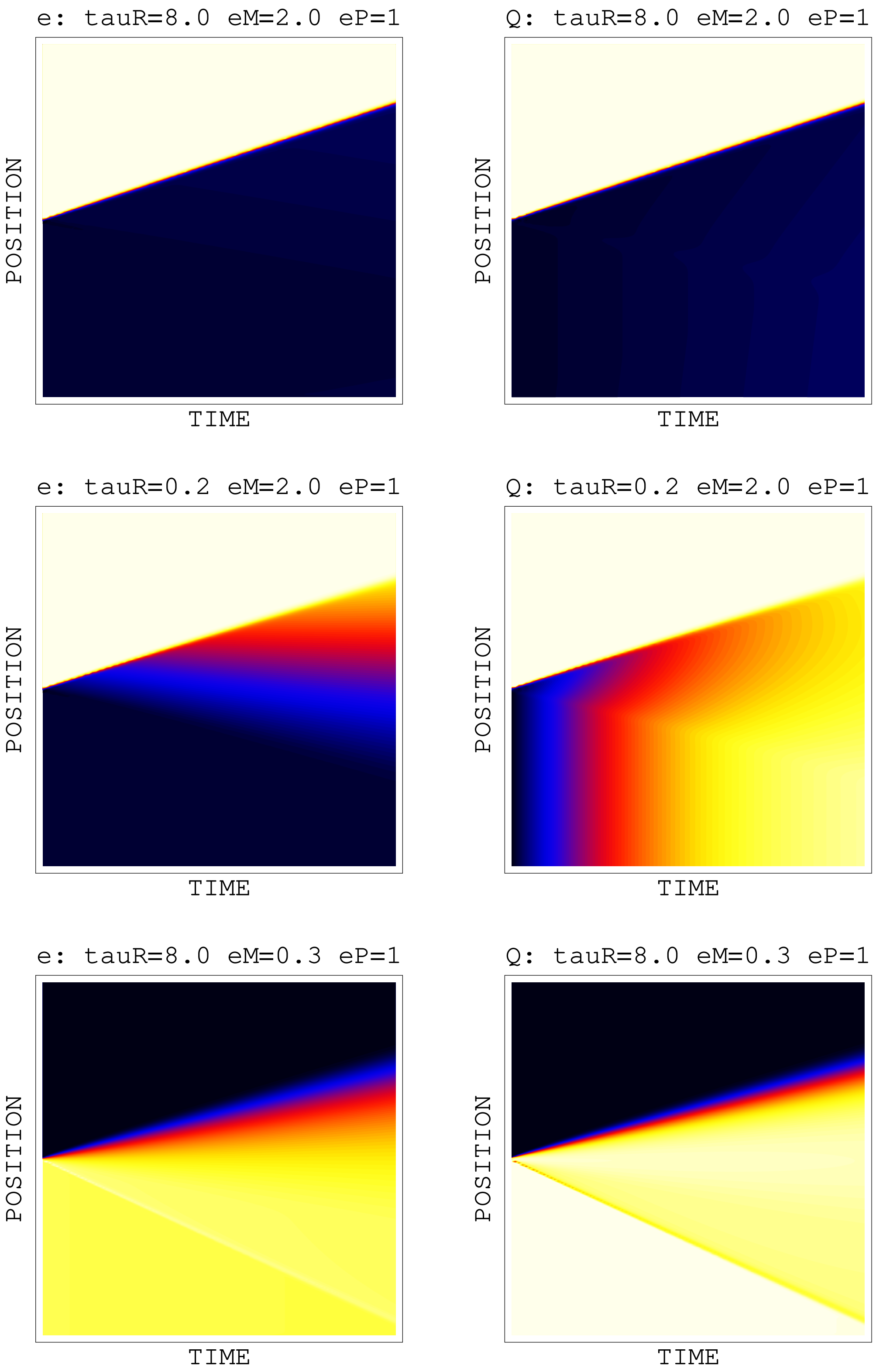

Figure 1: Fields of energy density and heat flux
for various inital conditions and relaxation times

5.3 Two interacting heat pulses

The next example for a pure IVP demonstrates the interaction of two heat pulses which leads to a large increase of the energy density at the collision point during a short time interval. Figure 2 represents the solution of the IVP for the initial data

$$e_0(x) = \begin{cases} 1 & , \quad x \leq 0.3 \\ 2 & , \quad 0.3 < x \leq 0.4 \\ 1 & , \quad 0.4 < x \leq 0.6 \\ 2 & , \quad 0.6 < x \leq 0.7 \\ 1 & , \quad x \leq 1 \end{cases} , \qquad Q_0(x) = \begin{cases} 0 & , \quad x \leq 0.3 \\ 1 & , \quad 0.3 < x \leq 0.4 \\ 0 & , \quad 0.4 < x \leq 0.6 \\ -1 & , \quad 0.6 < x \leq 0.7 \\ 0 & , \quad x \leq 1 \end{cases} . \tag{5.11}$$

The two contour plots of the first row show the two fields energy density e and heat flux Q within the time range $0 \leq t \leq 0.5$ and the space region $0 \leq x \leq 1$. The relaxation time is $\tau_R = 8$ and the time step $\tau_M = 0.005$. The light and dark colours correspond to small and large values of the fields, respectively, ranging from $e_{min} = 0.7884$, $Q_{min} = -1$ (light colour) to $e_{max} = 4.1384$, $Q_{max} = 1$ (black colour). The two curves in the second row show the given initial data. The third row depicts the energy density and the heat flux at time $t = 0.2$. In comparison to the initial curve we observe at the collision point $x = 0.5$ a large increase of the energy density e.

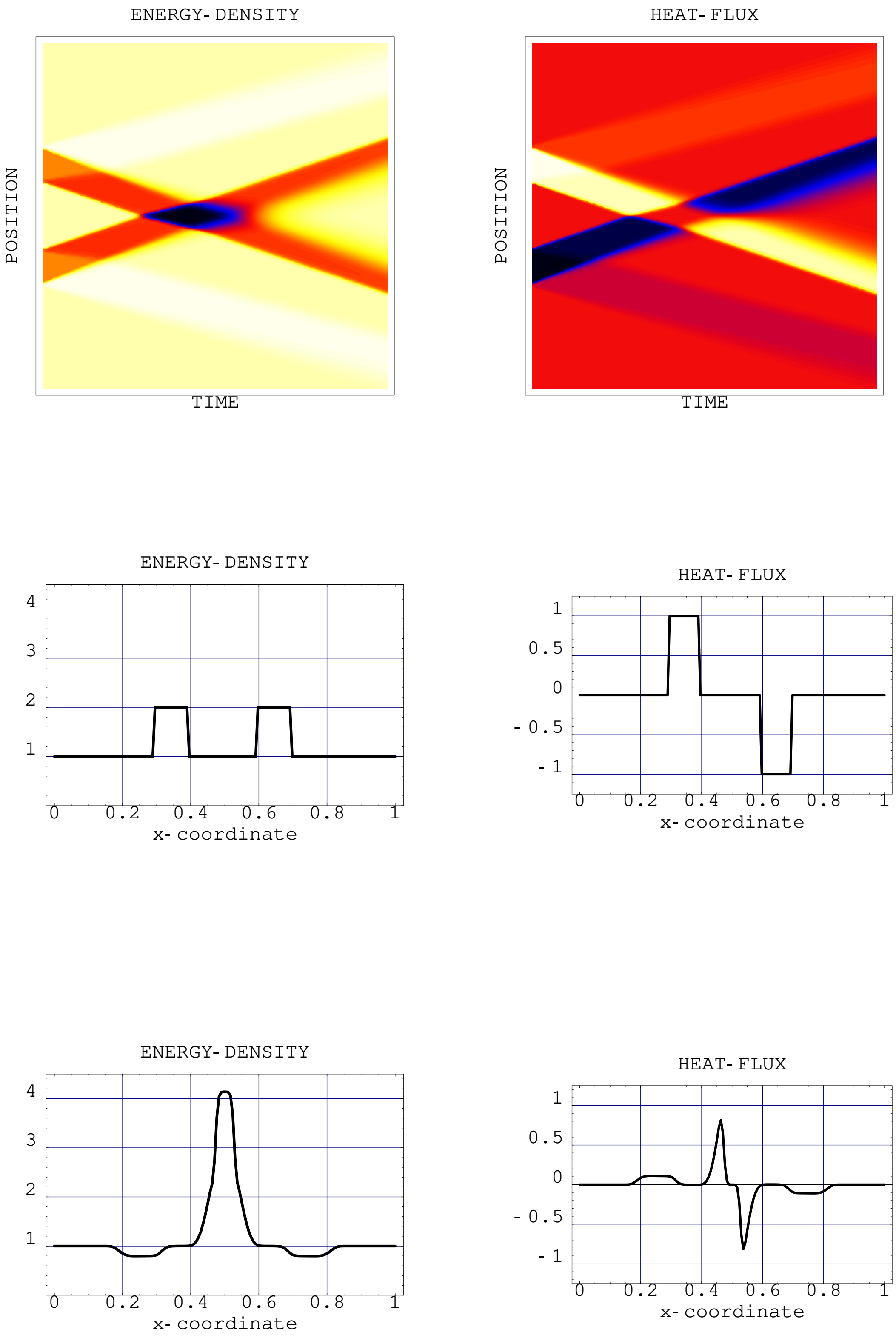

Figure 2: Two interacting heat pulses. First row: the fields of energy density and heat flux, second row: initial conditions, third row: spatial dependence of the fields at $t = 0.2$.

6 Representations for the Initial and Boundary Value Problem (IBVP)

6.1 Kinetic solution of the IBVP

Boundary value problems that are solved by integral representations of an underlying kinetic model confront us with a serious problem. For a discussion we consider a half space problem of a one dimensional crystal with a boundary at $x = 0$.

Our objective is the calculation of the fields of energy density and heat flux at location $\bar{x}$ and at time $0 < \bar{t} \leq \tau_M$. To this end we rely on an extension of representations (5.3) and (5.4). For every value of the integration variable $\nu \in [-1, 1]$ there is a micro characteristic

$$x(t) = \bar{x} - c\nu\left(\psi(\bar{t}) - \psi(t)\right) \tag{6.1}$$

through the point $(\bar{t}, \bar{x})$ which starts for $\nu < \nu_0$ from the initial line $t = 0$ and for $\nu > \nu_0$ from the boundary $x = 0$. The critical value

$$\nu_0 = \frac{\bar{x}}{c\psi(\bar{t})} > 0 \tag{6.2}$$

corresponds to the micro characteristic that originates at the point $(0, 0)$.

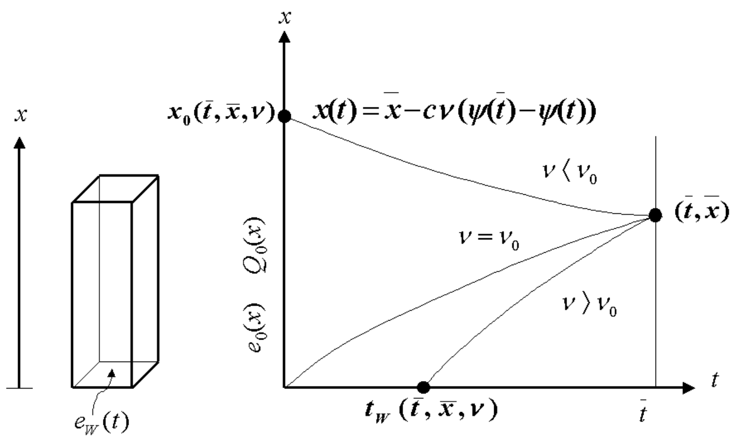

Figure 3: Micro characteristics relating $(\bar{t},\bar{x})$ to the initial- and boundary line

Figure 3 illustrates three selected micro characteristics and the functions

$$x_0(\bar{t}, \bar{x}, \nu) = \bar{x} - c\psi(\bar{t})\nu, \qquad t_W(\bar{t}, \bar{x}, \nu) = -\tau_R \ln\left[\exp\left(-\frac{\bar{t}}{\tau_R}\right) + \frac{\bar{x}}{c\,\tau_R\nu}\right], \tag{6.3}$$

which denote the intersections of the micro characteristics with the initial axes $t = 0$ and with the boundary $x = 0$, respectively. These play an important role for the following representation formulas.
We introduce the abbreviation

$$U(e, Q, \nu) = \frac{3}{2} \frac{e\,(4-F)^3}{F\,\left(1 - \frac{F}{4}\frac{Q}{ce}\nu\right)^4} \qquad \text{with} \qquad F = \frac{6}{1 + \sqrt{1 - \frac{3}{4}\left(\frac{Q}{ce}\right)^2}} \ , \tag{6.4}$$

and form the representation formula of the initial and boundary value problem (in the following abbreviated as IBVP) by means of two auxiliary functions $e_H(t)$ and $Q_H(t)$ which will be determined later on. To calculate the fields $e(\bar{t}, \bar{x})$ and $Q(\bar{t}, \bar{x})$ we write

$$\begin{aligned} e(\bar{t}, \bar{x}) \;&=\; \int_{-1}^{\nu_0} U(e_0(x_0(\bar{t}, \bar{x}, \nu)), Q_0(x_0(\bar{t}, \bar{x}, \nu)), \nu)\, d\nu \\ &+ \int_{\nu_0}^{1} U(e_H(t_W(\bar{t}, \bar{x}, \nu)), Q_H(t_W(\bar{t}, \bar{x}, \nu)), \nu)\, d\nu, \end{aligned} \tag{6.5}$$

$$\begin{aligned} Q(\bar{t}, \bar{x}) = \; c \exp\left(-\frac{\bar{t}}{\tau_R}\right) \; \Bigg[&\int_{-1}^{\nu_0} U(e_0(x_0(\bar{t}, \bar{x}, \nu)), Q_0(x_0(\bar{t}, \bar{x}, \nu)), \nu)\, \nu\, d\nu \\ &+ \int_{\nu_0}^{1} U(e_H(t_W(\bar{t}, \bar{x}, \nu)), Q_H(t_W(\bar{t}, \bar{x}, \nu)), \nu)\, \nu\, d\nu \Bigg] . \end{aligned} \tag{6.6}$$

The initial and boundary data are denoted by

$$e(0, x) = e_0(x), \qquad Q(0, x) = Q_0(x), \qquad e(t, 0) = e_W(t), \qquad Q(t, 0) = Q_W(t). \tag{6.7}$$

Note that either $(6.7)_3$ or $(6.7)_4$ must be prescribed. This is shown next.
The solution of the IBVP, i.e. the representations (6.5) and (6.6), must satisfy the following two continuity conditions at the boundary

$$\lim_{\bar{x} \to 0} e(\bar{t}, \bar{x}) = e_W(\bar{t}), \qquad \lim_{\bar{x} \to 0} Q(\bar{t}, \bar{x}) = Q_W(\bar{t}). \tag{6.8}$$

These read explicitly at any time t

$$e_W(t) = \int_{-1}^{0} U(e_0(x_0(t, 0, \nu)), Q_0(x_0(t, 0, \nu)), \nu)\, d\nu + \int_{0}^{1} U(e_H(t), Q_H(t), \nu)\, d\nu, \tag{6.9}$$

$$Q_W(t) = c\,\exp\left(-\tfrac{t}{\tau_R}\right)\left[\int\limits_{-1}^{0} U(e_0(x_0(t,0,\nu)),Q_0(x_0(t,0,\nu)),\nu)\,\nu\,d\nu \right. \tag{6.10}$$
$$\left. + \int\limits_{0}^{1} U(e_H(t),Q_H(t),\nu)\,\nu\,d\nu\right].$$

Here the auxiliary functions e_H and Q_H do no longer depend on the integration variable ν. Thus the integrals that contain e_H and Q_H can be carried out and the continuity conditions (6.9) and (6.10) turn out to be algebraic equations for e_H and Q_H.

We introduce the abbreviations

$$a = \frac{F_H}{4}\frac{Q_H}{c\,e_H}, \qquad f(a) = \frac{1}{2}\,\frac{a^2-3a+3}{a^2+3}(1+a)^3, \qquad g(a) = \frac{1}{4}\,\frac{3-a}{a^2+3}(1+a)^3, \tag{6.11}$$

and obtain from (6.9) and (6.10)

$$e_W(t) \;=\; e_H(t)f(a(t)) \;+\; \int\limits_{-1}^{0} U(e_0(x_0(t,0,\nu)),Q_0(x_0(t,0,\nu)),\nu)\,d\nu, \tag{6.12}$$

$$Q_W(t)\frac{\exp\left(\frac{t}{\tau_R}\right)}{c} \;=\; e_H(t)g(a(t)) \;+\; \int\limits_{-1}^{0} U(e_0(x_0(t,0,\nu)),Q_0(x_0(t,0,\nu)),\nu)\,\nu\,d\nu. \tag{6.13}$$

We conclude that the auxiliary functions $e_H(t)$ and $Q_H(t)$ are determined by two non-linear algebraic equations if the functions $e_W(t)$ and $Q_W(t)$ were given at the boundary.

However, this confronts us with a problem. For a discussion we assume for the moment that $e_W(t)$ and $Q_W(t)$ are prescribed independent of each other. Under this assumption we consider two cases in order to demonstrate that it leads to a contradiction and is thus not possible. In the first case we additionally assume that we could choose the auxiliary functions such that they coincide with the boundary data, i.e. $e_H = e_W$ and $Q_H = Q_W$. It follows that the algebraic equations (6.12) and (6.13) are not satisfied, i.e.

$$\lim_{\bar{x}\to 0} e(\bar{t},\bar{x}) \neq e_W(\bar{t}), \qquad \lim_{\bar{x}\to 0} Q(\bar{t},\bar{x}) \neq Q_W(\bar{t}). \tag{6.14}$$

In the second case we assume that e_H and Q_H follow from the algebraic system (6.12) and (6.13) for given e_W and Q_W. Here another contradiction appears because the quantity a is restricted to the range $[-1,+1]$ according to its definition (6.11).

However, the corresponding solution of the necessary continuity conditions (6.12) and (6.13) leads in general to values of a out of that range. We conclude that we cannot prescribe independently $e_W(t)$ and $Q_W(t)$.

We mention here an experimental consequence, whereupon e_W and Q_W cannot be given simultaneously. Either the temperature, i.e. e_W, is controlled at the wall or the wall is equipped with a generator of heat and thus the heat flux is prescribed.

To proceed the discussion we consider now exclusively the case that $e_W(t)$ but not $Q_W(t)$ is prescribed. Consequently, the function $Q_W(t)$ must also be calculated. We need one further condition that allows the determination of the auxiliary functions $e_H(t)$ and $Q_H(t)$ and of $Q_W(t)$. In addition to the two algebraic conditions (6.12) and (6.13) we found that it is necessary to require a third continuity condition for $0 < t \leq \tau_M$, namely

$$e_H(t) = e_W(t) \ , \tag{6.15}$$

which guarantees that the continuity conditions (6.8) are also satisfied in the limit $\tau_M \to 0$. For evaluation we use Newtons method in order to solve the resulting equation for $a(t)$, which is a combination of (6.12) and the third continuity condition (6.15)

$$1 - f(a(t)) = \frac{1}{e_W(t)} \int\limits_{-1}^{0} U(e_0(x_0(t,0,\nu)), Q_0(x_0(t,0,\nu)), \nu) \, d\nu \ . \tag{6.16}$$

Since $f(a)$ is monotonically increasing from $f(-1) = 0$ to $f(1) = 1$, a solution of (6.16) only exists whenever the right-hand side of (6.16) is in the range $[0, 1]$.

Finally we may now determine the auxiliary field $Q_H(t)$ according to the definition of $a = a(t)$

$$Q_H(t) = \frac{4c\, a(t)}{a(t)^2 + 3}\, e_H(t) \ . \tag{6.17}$$

The next two examples exhibit a surprising consequence of condition (6.15): Immediately after the initial time and after a sufficient number of maximizations of entropy were carried out, the boundary values e_W and Q_W are related to the initial data according to the Rankine-Hugoniot conditions.

6.2 Two explicit examples for IBVPs

The following numerical results serve to illustrate this observation and additionally record three nonlinear phenomena: a) the formation and steepening of shock fronts, b) the speed of shock fronts is apparently larger then $c/\sqrt{3}$,
c) the broadening of initial heat pulses at later times.

Figures 4 and 5 display the propagation of the heat pulse

$$e_W(t) = \begin{cases} 1 & , \quad t \leq 0 \\ 3 & , \quad 0 < t \leq 0.5 \\ 1 & , \quad t > 0.5 \end{cases} , \tag{6.18}$$

which is created at the lower boundary. The initial data are $e_0 = 1$ and $Q_0 = 0$.

In Figure 4 we consider the undamped case. The first row of Figure 4 shows the boundary data. Note that only $e_W(t)$ is prescribed but $Q_W(t)$ is calculated according to (6.15)-(6.17). The second and third row show the solution at times $t = 0.5$ and $t = 1.5$, respectively, for $0 \leq x \leq 1.5$.

We observe that the pulse front remains a shock moving with the speed $0.72\,c$, which is confirmed by the Dreyer-Seelecke condition (5.7). The rear side of the pulse changes into a rarefaction wave. Thereby it comes to a broadening, even if there is no damping.

Figure 5 illustrates the effect of large damping due to the relaxation time $\tau_R = 0.5$. In contrast to the undamped case, the heat flux may become negative here. The last row of Figure 5 shows the fields e and Q at time $t = 1.5$ exhibiting a large broadening of the rear side of the initial pulse. Note that this phenomenon cannot be observed in the undamped case, although a rarefaction wave appears at the rear side of the pulse here. Furthermore the solution decays rapidly to an equilibrium state.

In the last example which is represented in Figure 6 we create the periodic heat signal

$$e_W(t) = 2 - \cos(8\pi\, t) \tag{6.19}$$

at the lower boundary. The initial data are again $e_0 = 1$ and $Q_0 = 0$. The left and right columns show the effect of zero damping ($\tau_R \to \infty$) and high damping ($\tau_R = 0.5$), respectively. The first two rows of Figure 6 depict the boundary data. Note again that only $e_W(t)$ is prescribed but $Q_W(t)$ is calculated according to (6.15)-(6.17). Surprisingly even in this example $Q_W(t)$ meets the value Q that we obtain by the Dreyer-Seelecke condition with $e_+(t) = e_0 = 1$, $Q_+(t) = Q_0 = 0$ and $e_-(t) = e_W(t)$, at least in the undamped case. The damped case requires a more detailed study. The last two rows illustrate the solution at time $t = 1.5$ for $0 \leq x \leq 1.5$. The formation and steepening of shock fronts is clearly visible. As before, we observe regions in space with a negative heat flux which is due to the damping.

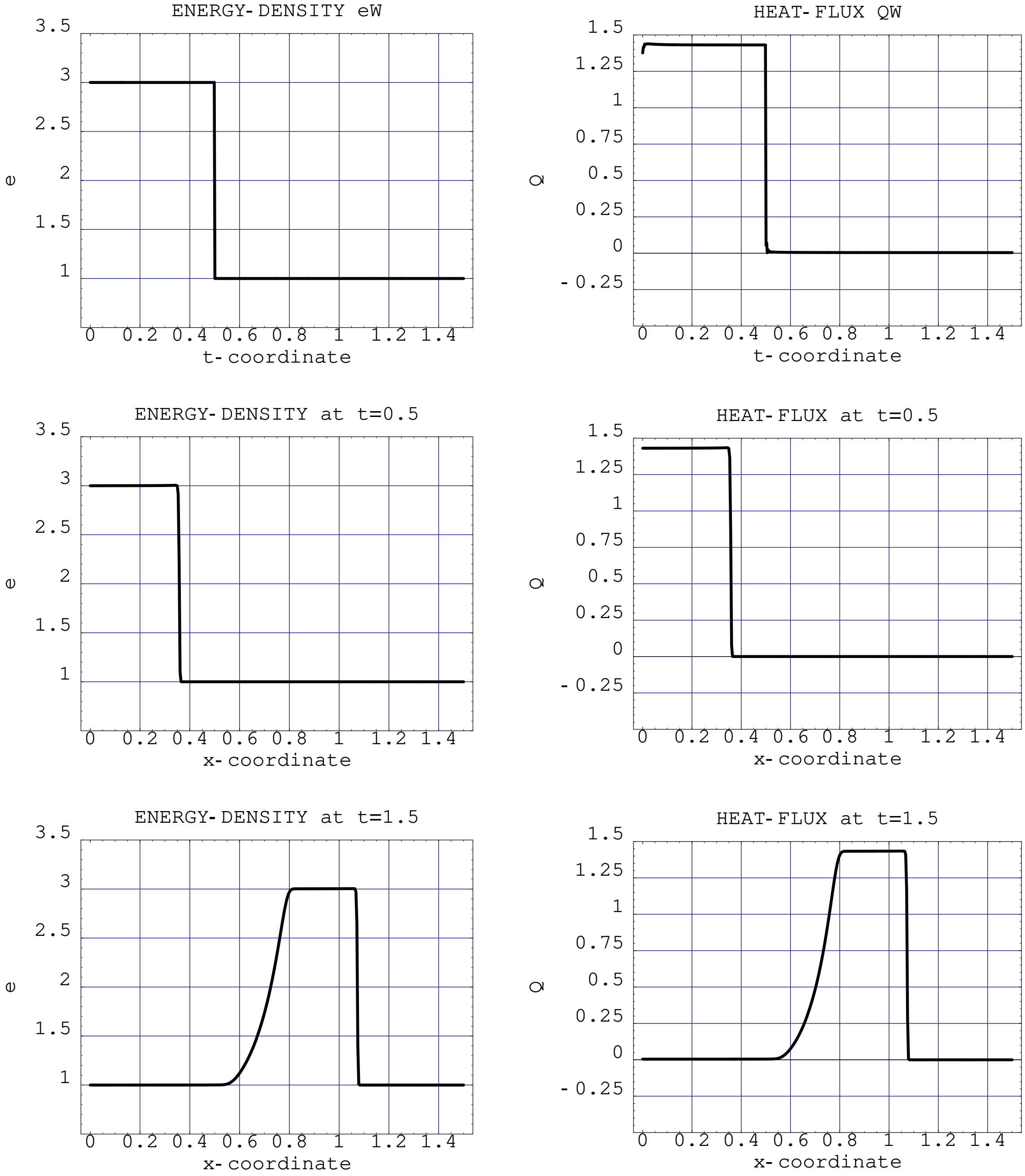

Figure 4: Creation of a heat pulse for $\tau_R \to \infty$. First row: boundary data for the energy density and the resulting heat flux, second and third row: energy density and heat flux at time $t = 0.5$ and at $t = 1.5$, respectively.

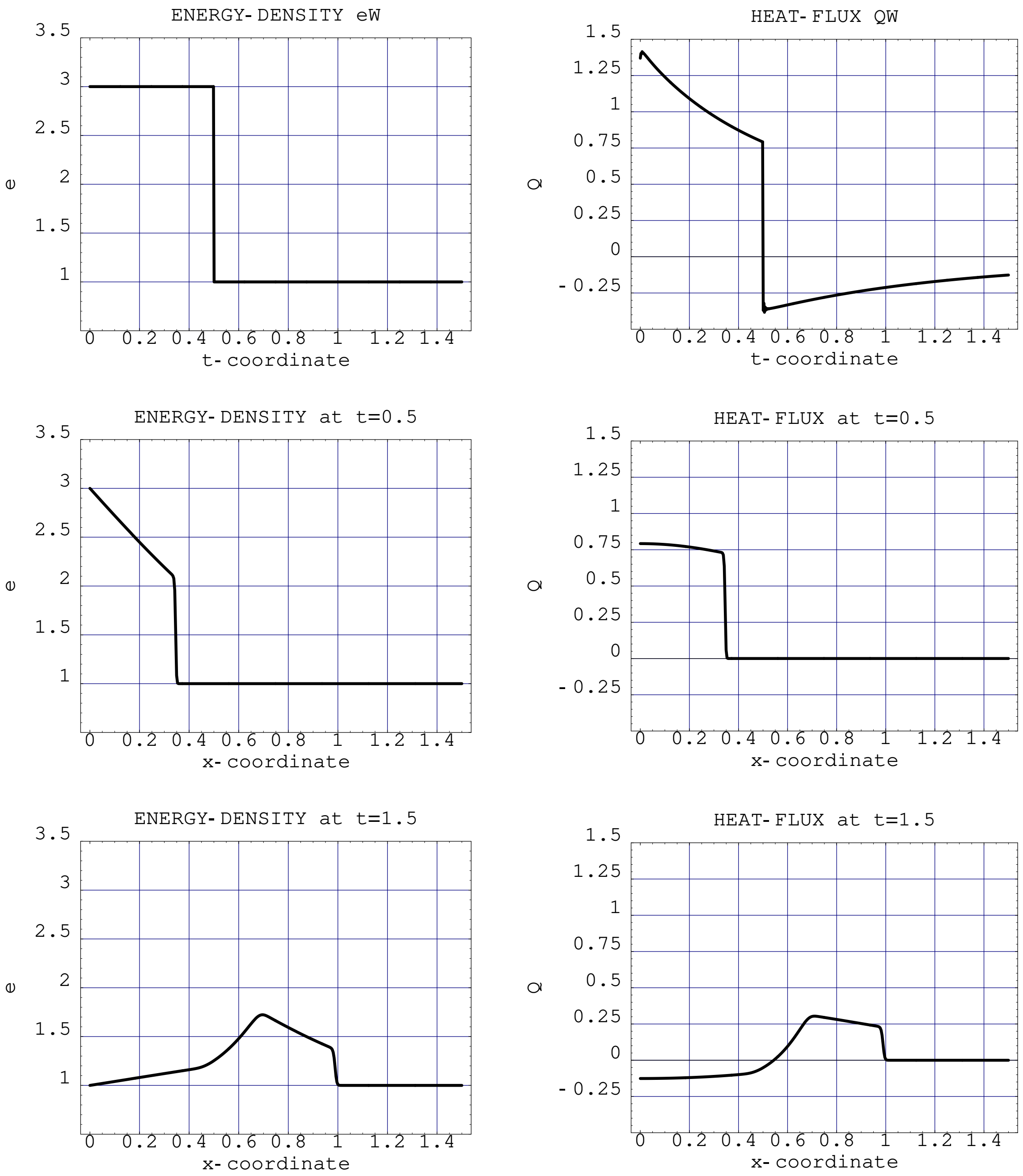

Figure 5: Creation of a heat pulse for $\tau_R = 0.5$. First row: boundary data for the energy density and the resulting heat flux, second and third row: energy density and heat flux at time $t = 0.5$ and at $t = 1.5$, respectively.

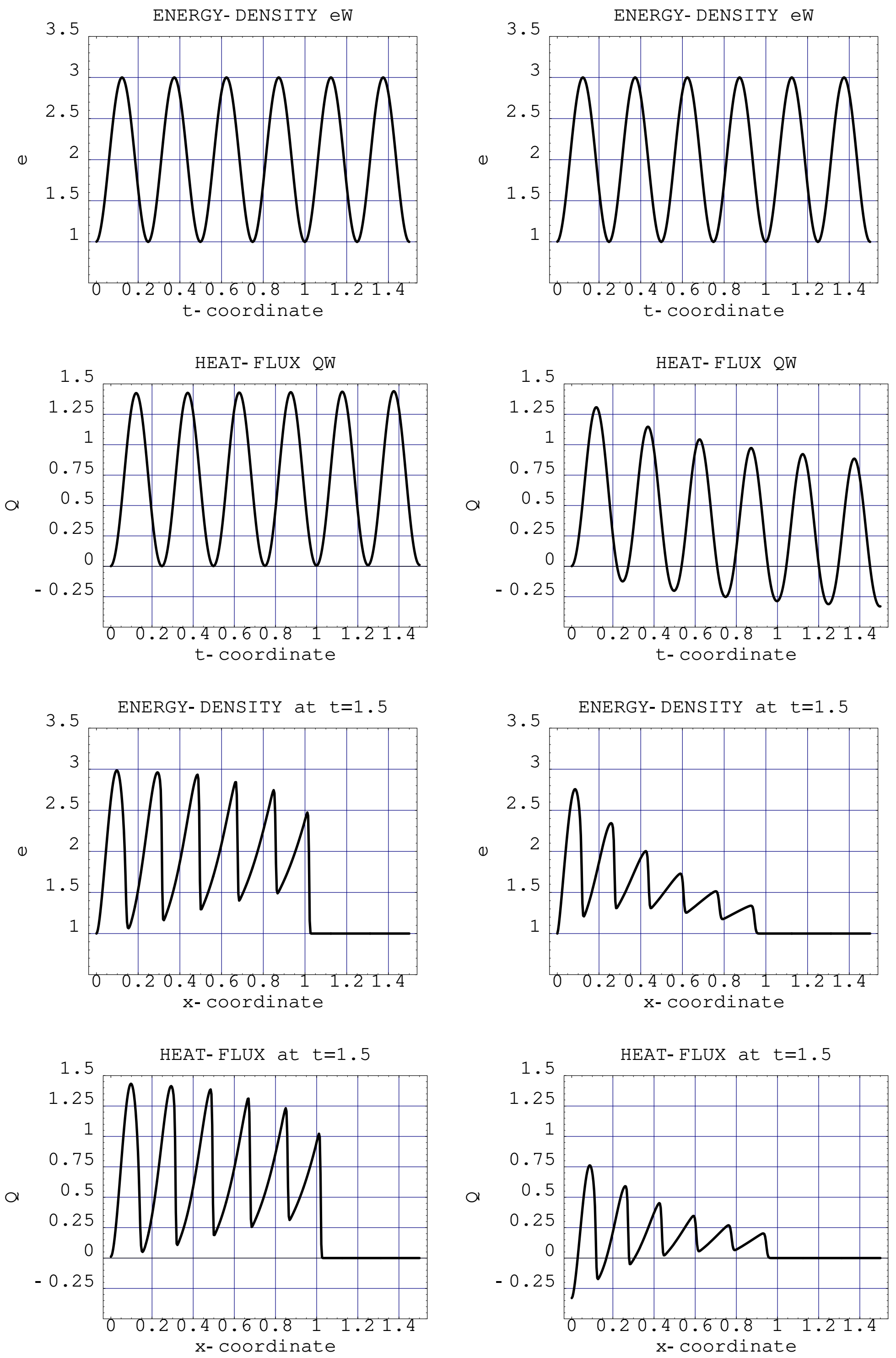

Figure 6: A periodic boundary condition. Left and right column: $\tau_R \to +\infty$ and $\tau_R = 0.5$, respectively. First and second row: boundary data for the energy density and the resulting heat flux, third and fourth row: energy density and heat flux at time $t = 1.5$.

6.3 The linear limit

In this section we choose initial- and boundary data so that the solution of the non-linear system (5.5) agrees approximately with the solution of the linear limit. The latter is obtained from the full system by neclegting terms of the order Q^2. For simplicity we set $c = \sqrt{3}$ and consider the case $\tau_R \to \infty$.

The initial data are

$$e_0(x) = \begin{cases} 1 & , \quad 0.0 < x \leq 0.4 \\ 1+\epsilon & , \quad 0.4 < x \leq 0.8 \\ 1 & , \quad x > 0.8 \end{cases} , \qquad Q_0(x) = \begin{cases} 0 & , \quad 0.0 < x \leq 0.4 \\ -\epsilon & , \quad 0.4 < x \leq 0.8 \\ 0 & , \quad x > 0.8 \end{cases} . \tag{6.20}$$

Here $\epsilon > 0$ is a fixed positive constant; in particular we choose $\epsilon = 0.01$. At the boundary we prescribe the energy density to be

$$e_W(t) = 1 \ . \tag{6.21}$$

The solution of this problem according to the representation formulas (6.5) and (6.6) can be read off from Figure 7 for $0 \leq t \leq 1$ and $0 \leq x \leq 1$.

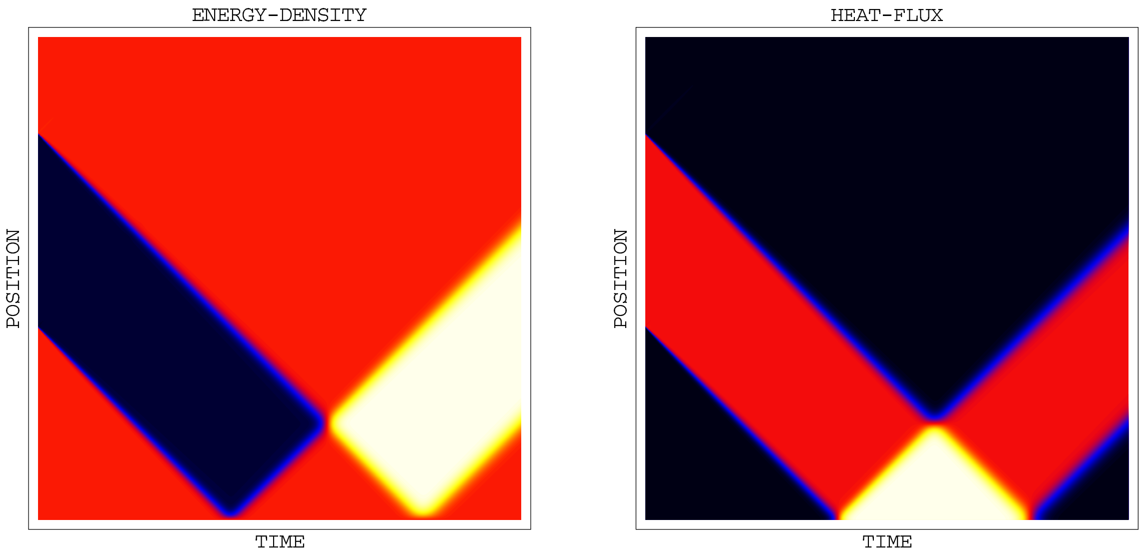

Figure 7: The nonlinear solution of the IBVP for $\varepsilon = 0.01$

The Figure reveals the well known behaviour of a linear wave equation because ϵ was chosen so that terms of order Q^2 show no influence. Furthermore we observe that the prescribed constant boundary data $e_W = 1$ causes a reflection of the incoming wave from the initial line.

In order to establish agreement with the linear theory we will compare the solution of the non-linear system (5.5) in Figure 7 with the solution of its linearized form that we study now. The linearized version of (5.5) reads

$$\int_{\partial\Omega} (e\,dx \;-\; Q\,dt) = 0\ , \qquad \int_{\partial\Omega} (Q\,dx \;-\; e\,dt) = 0\ . \tag{6.22}$$

(6.22) leads to the following system of wave equations:

$$\frac{\partial e}{\partial t} \;+\; \frac{\partial Q}{\partial x} = 0\ , \qquad \frac{\partial Q}{\partial t} \;+\; \frac{\partial e}{\partial x} = 0\ . \tag{6.23}$$

Across a shock with velocity V_s we obtain from (6.22) the jump conditions

$$V_s\,(e_+ - e_-) = Q_+ - Q_-\ , \qquad V_s\,(Q_+ - Q_-) = e_+ - e_-\ , \tag{6.24}$$

These equations immediately imply $V_s = +1$ or $V_s = -1$, which is a well known result. In the following we use the jump conditions (6.24) in order to construct the analytical solution of the IBVP from above.

Figure 8 shows the piecewise constant analytical solution of the linear problem. The various regions with constant states (e, Q) are bounded by jumps with slopes $+1$ and -1 or by the t- and x-axis, respectively.

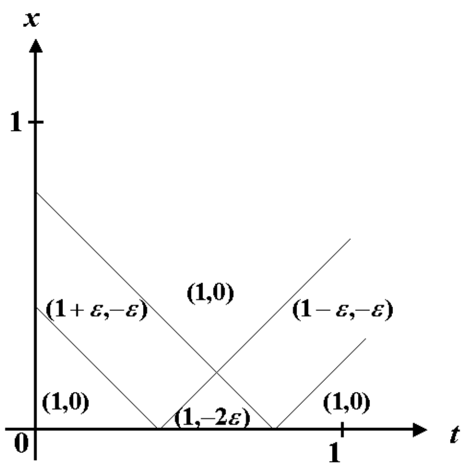

Figure 8: The analytical linear solution of the IBVP for $\varepsilon = 0.01$

Due to the small variation of the initial data there is good agreement between the nonlinear numerical solution of Figure 7 and the linear analytical solution of Figure 8. Note that the light colors in Figure 7 correspond to small values of the fields while large values are indicated by dark colors.

6.4 The stationary boundary value problem

Finally we study the analytical solution of the stationary boundary value problem. As before we consider the one-dimensional case. We reduce the local three-dimensional system (3.10) to the stationary one-dimensional case and obtain

$$\frac{d}{dx}Q = 0\ , \qquad \frac{d}{dx}(c^2\,N) = -\frac{1}{\tau_R}\,Q\ , \qquad N = \frac{5}{3}e - \frac{4\,e}{3}\sqrt{1-\frac{3}{4}\left(\frac{Q}{c\,e}\right)^2}\ , \tag{6.25}$$

where $e = e(x)$, $Q = Q(x)$ for $0 \leq x \leq L$. We prescribe values for e at the upper and lower boundary, viz.

$$e_- = e(0)\ , \quad e_+ = e(L). \tag{6.26}$$

The constant Debye velocity is again $c = 1$. $(6.25)_1$ implies that Q =constant, whereas $(6.25)_2$ leads to the algebraic equation

$$\frac{5}{3}\,e - \frac{4}{3}\sqrt{e^2 - \frac{3}{4}Q^2} = \gamma - \frac{x}{\tau_R}\,Q. \tag{6.27}$$

The boundary conditions at $x = 0$ and at $x = L$ are used for the determination of the integration constants γ and Q

$$\frac{5}{3}\,e_- - \frac{4}{3}\sqrt{e_-^2 - \frac{3}{4}Q^2} = \gamma, \qquad \frac{5}{3}\,e_+ - \frac{4}{3}\sqrt{e_+^2 - \frac{3}{4}Q^2} = \gamma - \frac{L}{\tau_R}\,Q. \tag{6.28}$$

Subtracting these equations leads to a single equation for Q, namely

$$\frac{5}{3}\,(e_- - e_+) - \frac{4}{3}\left(\sqrt{e_-^2 - \frac{3}{4}Q^2} - \sqrt{e_+^2 - \frac{3}{4}Q^2}\right) - \frac{LQ}{\tau_R} \;=\; 0\ , \tag{6.29}$$

which may be solved by Newtons method.

The other constant γ results then immediately from $(6.28)_1$. With known values for Q and γ we may solve the equation for the energy density e in (6.27). It turns out that the solution only admits the "+" sign and reads

$$e(x) \;=\; -\frac{5}{3}\left(\frac{Qx}{\tau_R} - \gamma\right) \;+\; \sqrt{\frac{16}{9}\left(\frac{Qx}{\tau_R} - \gamma\right)^2 - \frac{4}{3}Q^2}. \tag{6.30}$$

The same representation can be used in order to solve the mixed boundary value problem for given e_- and $Q = Q_+$. In this case γ can be read off from the equation $(6.28)_1$.

References

[1] W. Dreyer, M. Kunik, *The Maximum Entropy Principle Revisited.* WIAS-Preprint No. 367 (1997). Cont. Mech. Thermodyn. **1** (1999).

[2] W. Dreyer, M. Kunik, *Reflections of Eulerian shock waves at moving adiabatic boundaries.* WIAS-Preprint No. 383 (1997). Monte Carlo Methods and Applications **4** (1998), 231-252.

[3] B. Pertame, *The kinetic approach to systems of conservation laws, recent advances in partial differential equations*, editors M.A. Herrero and E. Zuazua, Wiley and Mason (1994), 85-97.

[4] W. Dreyer, H. Struchtrup, *Heat pulse experiments revisited.* Cont. Mech. Thermodyn. **5** (1993), 3-50.

[5] I. Müller, T. Ruggeri, *Rational Extended Thermodynamics.* 2nd Edition, Springer Tracts in Natural Philosophy, Springer New York, 1998.

[6] W. Dreyer, S. Seelecke, *Entropy and causality as criteria for the existence of shock waves in low temperature heat conduction.* Cont. Mech. Thermodyn. **4** (1992), 23-36

[7] W. Dreyer, *Maximization of the Entropy in Non-Equilibrium.* J. Phys. A.: Math. Gen. **20** (1987), 6505-6517.

[8] G. Boillat, T. Ruggeri, *Moment equations in the kinetic theory of gases and wave velocities.* Cont. Mech. Thermodyn., **9** (1987).

[9] W. Larecki, S. Piekarski, *Phonon gas hydrodynamics based on the maximum entropy principle and the extended field theory of a rigid conductor of heat.* Arch. Mech. **43** (1992), pp 163.